Measurement of Velocity Fluctuations and Overpressure of Spherical Shock Wave in Grid Turbulence

K. Inokuma, S. Nishio, T. Watanabe, K. Nagata, Akihiro Sasoh, and Y. Sakai

Abstract Velocity fluctuations of grid turbulence and overpressure of spherical shock wave are measured simultaneously in wind tunnel experiments. The experiments are conducted for four different conditions of grid turbulence, where the turbulent intensity and the length scales are different. Probability density functions (PDFs) of the velocity fluctuation and the peak-overpressure fluctuation measured on the wall are calculated in each experimental condition, and both follow the Gaussian profile. In this study, the instantaneous spatial distributions of turbulent velocity are estimated with the Taylor hypothesis. Correlation coefficients are calculated for the peak-overpressure fluctuation and the spatial distribution of the low-pass filtered turbulent velocity fluctuation to evaluate the relation between them. The positive correlation is found for the velocity fluctuation at the location away from the wall. The correlation calculated for a wide range of the cutoff length shows that the turbulent motions of the order of the integral length scale have large influences on the peak-overpressure fluctuation.

1 Introduction

The interaction between shock wave (SW) and turbulence is a ubiquitous problem in science (e.g., star formations in galaxies [1] and inertial confinement fusion [2]) and in engineering applications (e.g., sonic boom generated by supersonic transports [3]). The post-SW overpressure modulation observed as a peak-overpressure fluctuation induced by the effects of turbulence is known to be one of the most important phenomena of this problem [4–7].

Despite the importance of this problem in such various fields, the detailed mechanisms of the modulation are not clear yet because turbulent velocity and the SW overpressure were not measured simultaneously in most previous studies. For

K. Inokuma (✉) · S. Nishio · T. Watanabe · K. Nagata · A. Sasoh · Y. Sakai
Department of Mechanical Systems Engineering, Nagoya University, Nagoya, Japan
e-mail: inokuma@nagoya-u.jp

A. Sasoh et al. (eds.), *31st International Symposium on Shock Waves 1*,
https://doi.org/10.1007/978-3-319-91020-8_142

further investigations, it is necessary to reveal the relation between the instantaneous spatial distributions of turbulent velocity and the SW overpressure modulation.

In this study, we perform simultaneous measurements of the velocity fluctuations of grid turbulence and the spherical SW overpressure in wind tunnel experiments. Taylor hypothesis is used to estimate the spatial distributions of velocity fluctuations. The modulation of the SW overpressure is investigated in relation to the estimated spatial profile of velocity.

2 Methods

The experimental setup is shown in Fig. 1a. A square grid with a mesh size M (solidity, 0.36) is installed at the entrance to the test section of the wind tunnel (the detail of wind tunnel can be seen in [6, 8]) to generate turbulent velocity field. We use two square grids with $M = 50$ mm and 100 mm. On the other hand, a spherical SW is ejected vertically downward from an open end of a tube using a quick piston valve. The total length and the inner diameter of the tube are 3.4 m and 23.3 mm, respectively. The spherical SW generator was also used in our previous studies [6]. Between the grid and the open end of the shock tube, we install a measurement plate with the thickness of 5 mm, on which a piezoelectric pressure transducer (PCB Piezotronics Inc. 113B27) and an I-type hot-wire probe (Dantec Dynamics 55P11) are mounted (see Fig. 1a) for the measurements of overpressure $P(t)$ and velocity $U(t)$. The measurement plate is fixed 75 mm above the wall of the wind tunnel to prevent the boundary layer from affecting the measurement. The shock Mach number is $M_{S0} = 1.004$ on the measurement plate. Table 1 summarizes the experimental conditions including turbulence characteristics at the measurement location. Further detail of grid turbulence studied here can be found in [8]. The signals of $P(t)$ and $U(t)$ are sampled with the oscilloscope (Yokogawa DL750)

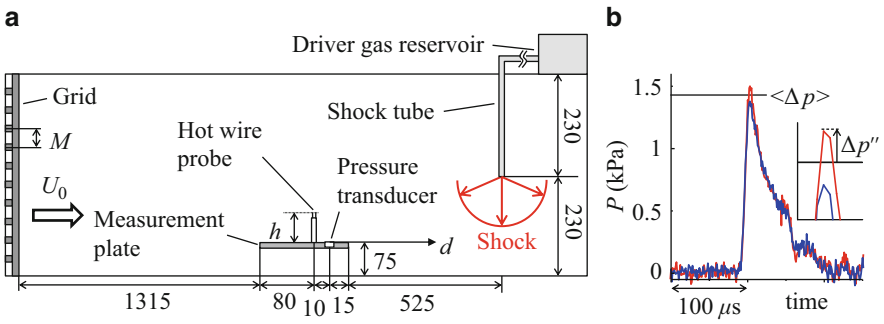

Fig. 1 (**a**) Experimental setup (lengths are shown in mm). (**b**) Examples of time histories of overpressure P for M100-U10 (red/blue line shows strong/weak case) and the ensemble average of peak overpressure $\langle \Delta p \rangle$ and peak-overpressure fluctuation $\Delta p'' = \Delta p - \langle \Delta p \rangle$ are also shown

Table 1 Experimental conditions of the spherical SW and grid turbulence interaction experiments, where $Re_M = UM/\nu$ is the mesh Reynolds number (ν, the kinematic viscosity; M, the mesh size; U_0, the streamwise mean velocity); the turbulence statistic at the measurement location is shown for the rms streamwise velocity fluctuation $u_{\rm rms}$, Kolmogorov microscale η, Taylor microscale λ, and longitudinal integral length scale L_u calculated from the longitudinal autocorrelation function (the definitions of scales can be seen in [8]); and the table also includes the rms peak-overpressure fluctuation $p_{\rm rms}$ obtained in the experiments

Case	M50-U10	M50-U20	M100-U10	M100-U20
Symbol	$\triangle$ (blue)	$\circ$ (green)	∇ (black)	$\square$ (red)
M (mm)	50	50	100	100
U_0 (m/s)	10	20	10	20
$Re_M \times 10^{-4}$	3.35	6.7	6.7	13.4
η (mm)	0.198	0.134	0.163	0.112
λ (mm)	3.92	3.75	3.91	3.78
L_u (mm)	27.5	48.1	54.3	64.3
$u_{\rm rms}$ (m/s)	0.387	0.798	0.568	1.17
$p_{\rm rms}/\langle\Delta p\rangle$	0.0269	0.0620	0.0338	0.0703

at the sampling rate of 1 MHz. The SW generator and the measurement system are controlled by a computer: the sampling is started 50 ms before the SW is ejected from the open end. The velocity measurement height h defined in Fig. 1a is ranged from 15 to 125 mm. In each measurement condition, 500 runs of the SW ejection into the grid turbulence were conducted for the statistical analysis. We also confirmed that 300 runs were enough to obtain the results discussed below.

Figure 1b shows examples of time histories of P. The peak overpressure Δp is the increase in P due to the SW defined with the peak value of P. $\Delta p''$ $(=\Delta p - \langle\Delta p\rangle)$ is the fluctuation of Δp from $\langle\Delta p\rangle$. Here, $\langle\ \rangle$ denotes the ensemble average of all runs of the SW. We analyze Δp in relation to $U(t)$ measured before the SW reaches the measurement plate. Table 1 also shows the rms values of the velocity fluctuation $u(t)=U(t)-U_0$ and of the peak-overpressure fluctuation $\Delta p''$, denoted as $u_{\rm rms}$ and $p_{\rm rms}$, respectively. We can find that $p_{\rm rms}$ increases with $u_{\rm rms}$ which is consistent with previous studies [4, 6, 7].

The turbulence past the probe is advected downstream by the mean flow. The spatial distribution of the velocity $U(d)$ at the probe height h can be estimated from $U(t)$ with the Taylor hypothesis, where d is the streamwise distance from the pressure transducer (see Fig. 1a). Since the fluid motion is much slower than the SW, the turbulence can be assumed to be frozen and hardly changes while the SW is propagating. This enables us to estimate the velocity distribution at the moment when the SW is ejected. The decay of grid turbulence is not important in the range of d considered here because the measurement location is far from the grid, while turbulence intensity changes with a power law of the streamwise distance from the grid [8].

The SW propagates upstream through the turbulence whose velocity profile at h is represented by $U(d)$ and reaches the pressure transducer location. We apply the low-pass filter with a cutoff length Δd to the velocity as $\overline{U}\,(d, \Delta d)\ =$

$(1/\Delta d)\int_{-\Delta d/2}^{\Delta d/2} U\,(d+\delta)\,\mathrm{d}\delta$, which is the velocity of motions in scales larger than Δd at the location d. This low-pass filtering is used for investigating the scale dependence of the pressure modulation by the turbulence.

The correlation coefficient defined with the ensemble average is calculated for $\Delta p''$ and $\overline{u}\,(d,\Delta d) = \overline{U}\,(d,\Delta d) - U_0$ as $R\,(d,\Delta d) = \langle \overline{u}\Delta p''\rangle / \sqrt{\langle(\overline{u})^2\rangle\langle(\Delta p'')^2\rangle}$ to evaluate the relation between the turbulence velocity fluctuation and the peak-overpressure fluctuation. This correlation coefficient is computed at all of the velocity measurement height h.

3 Results

Probability density functions (PDFs) of the velocity fluctuation and the peak-overpressure fluctuation, normalized by their rms values, are shown in Fig. 2a, b, respectively. We can find that both follow the Gaussian profile.

Figure 3 shows an example of the scatterplot of the velocity fluctuation $\overline{u}\,(d,\Delta d)\,/U_0$ and the peak-overpressure fluctuation $\Delta p''/\langle\Delta p\rangle$ at the location where the highest value is obtained for the correlation coefficient $R(d,\Delta d)$ in the case M100-U10. The scatterplot confirms that there exists positive correlation between the velocity and the peak-overpressure fluctuation.

We consider the set of $(d,\Delta d)$ for which the highest correlation coefficient R is obtained in all cases in Table 1. Hereafter, Δd_P denotes the value of Δd with the highest correlation. Δd_P is related to the length scale of turbulent motions which is the most effective to the modulation of the peak overpressure. In Fig. 4, $\Delta d_P/L_u$ is plotted against $M_\mathrm{T}/M_\mathrm{S0}$ ($M_\mathrm{T} = u_\mathrm{rms}/a$, the turbulent Mach number; a, the sound speed in front of the SW). We can find that Δd_P are of the order of the integral

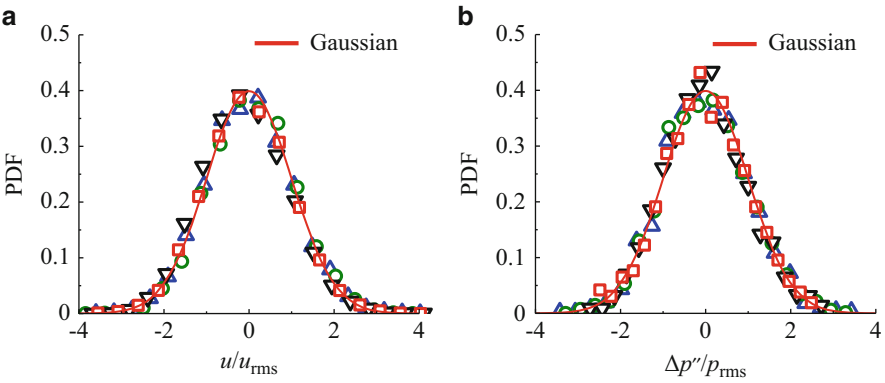

Fig. 2 PDFs of (**a**) velocity fluctuation u/u_rms and (**b**) peak-overpressure fluctuation $\Delta p''/p_\mathrm{rms}$; red line shows the Gaussian profile; see Table 1 for symbols

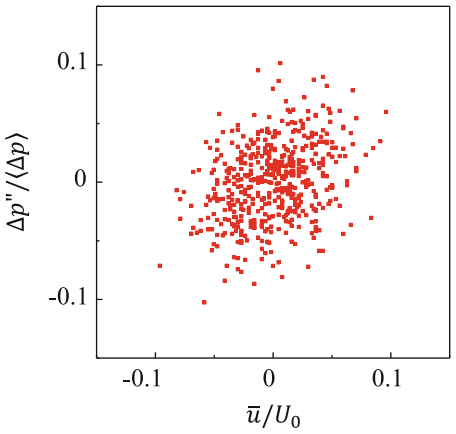

Fig. 3 Example of scatterplot of velocity fluctuation $\overline{u}\,(d, \Delta d)\,/\,U_0$ and peak-overpressure fluctuation $\Delta p''/\langle\Delta p\rangle$ of M100-U10, $h = 50$ mm, $(d, \Delta d) = (173$ mm, 162 mm); $R(d, \Delta d) = 0.330$

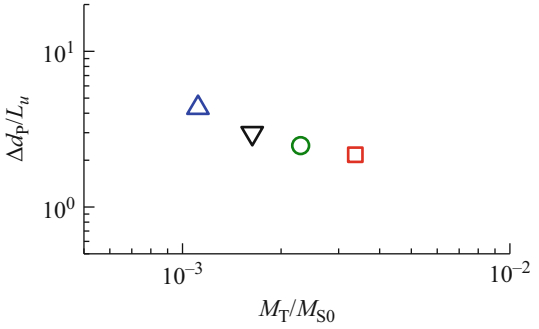

Fig. 4 Relation between $\Delta d_P/L_u$ and M_T/M_{S0}; see Table 1 for symbols

length scale, suggesting that the large scale of turbulent motions is related to the peak-overpressure modulation. It is also found that $\Delta d_P/L_u$ decreases as M_T/M_{S0} increases.

4 Conclusions

In this study, we simultaneously measured the flow velocity and the overpressure of the SW in grid turbulence where the spherical SW propagates. PDFs of the velocity fluctuation and the peak-overpressure fluctuation follow the Gaussian profile. The correlation coefficients calculated for the velocity and the peak-overpressure fluctuation confirm that the turbulent velocity is positively correlated to the peak-overpressure fluctuation and that the peak-overpressure modulation is induced by the turbulent motions at large scale.

Acknowledgments The authors would like to thank Dr. Y. Ito (Nagoya University) for his help and valuable comments to this study. Part of this study is supported by JSPS KAKENHI (No. 25289030).

References

1. M.-M. Mac Low, R.S. Klessen, Rev. Mod. Phys. **76**, 125 (2004)
2. V.A. Thomas, R.J. Kares, Phys. Rev. Lett. **109**, 075004 (2012)
3. C.B. Pepper et al., A review of the effects of aircraft noise on wildlife and humans, current control mechanisms, and the need for further study. Environ. Manag. **32**, 418 (2003)
4. B. Lipkens, D.T. Blackstock, J. Acoust. Soc. Am. **103**, 148 (1998)
5. O.I. Dokukina et al., Pressure fluctuations within a turbulent gas flow and their interaction with a shock wave. Mosc. Univ. Phys. Bull. **68**, 118 (2013)
6. A. Sasoh et al., Statistical behavior of post-shock overpressure past grid turbulence. Shock Waves **24**, 489 (2014)
7. J.H. Kim et al., Modulations of a weak shock wave through a turbulent slit jet. Shock Waves **20**, 339 (2010)
8. T. Kitamura et al., On invariants in grid turbulence at moderate Reynolds numbers. J. Fluid Mech. **738**, 378 (2014)